

---

# Mechanical investigations of two repair mortars and repaired system

Amjad Mallat<sup>1</sup>, Abdenour Alliche<sup>2\*</sup>

<sup>1</sup>CNRS Liban, P.O. Box 11-8281, Ryad El Solh 11 07 2260, 59 Zahia Selman Street, Beirut, Lebanon

<sup>2</sup>UPMC Univ. Paris 6, UMR 7190, Institut Jean Le Rond d'Alembert, F-75005 Paris France

[\\*abdenour.alliche@upmc.fr](mailto:abdenour.alliche@upmc.fr)

---

*ABSTRACT: The mechanical behavior of two repair mortars was investigated. The first one is a fiber reinforced lime-based mortar, which contains thickening agent and limestone additions. The second one is a fiber reinforced ordinary mortar, which contains a small quantity of silica fume and additives. Mechanical tests shows the influence of the surface roughness and moisture conditions on the bond strength.*

*RESUME : Deux mortiers de réparation ont été étudiés. le premier est un matériau renforcé de fibre et contenant un agent épaississant, le second mortier contient des ajouts d'additif dont la fumée de silice. Les résultats des essais mécaniques montrent clairement l'influence de l'état de surface et de l'humidité sur l'adhérence de l'interface entre le substrat et le matériau de réparation.*

*KEYWORDS: Repair mortars, Mechanical behavior, Interfacial zone, Bond strength.*

*MOTS CLES : Mortiers de réparation, comportement mécanique, interface, adhérence.*

---

## 1. Introduction

In recent years, repair refurbishment and maintenance of concrete structures have become a significant part of the total cost of construction worldwide (Mangat and Limbachia 1997). Different repair methods and materials are currently used to overcome damage in deteriorated structures. The choice is a function of both the physico-chemical and the mechanical properties of the substrate. Fiber-reinforced mortar is one of the materials widely used to repair old concrete. In the fiber-reinforced mortar, fibers are usually discontinuous and randomly distributed throughout the composite. In the hardened mortar, fibers prevent the microcracks from developing into macrocracks (Pascal *et al.*, 2004). In addition, these fibers bridge and therefore hold together the existing macrocracks, thus reinforcing the concrete against failure. The property enhancement of fiber-reinforced mortar can be largely attributed to the crack bridging forces provided by the fibers, which limit crack opening and distribute the stresses to the nearby matrix, thus suppressing strain localization. Consequently, the strength and strain capacity of the composite are increased appreciably. Under current practice, there are no standard procedures for the design of patch repairs. Design is usually based on the experience of specialist contractors and when the selection of repair materials is made, emphasis is normally given to their relative short-term properties such as strength and bond and early age plastic shrinkage/expansion. Although these properties indicate the immediate performance of the repair, they give little information on its long-term performance. Therefore, there is an important need for recognizing and understanding the properties evolution of repair materials, which are of significance to the subsequent structural behaviors of repaired concrete members. An important factor for the success of repair works in concrete structures is to realize sufficient bonding between the repair material and the substrate (Li and Xiong. 2001, Jolio and al. 2004, Emmons 1994). In this study, bonding capacity of the repair mortars to the substrate was investigated. For this purpose, a range of surface roughness with various substrate moisture conditions was studied by slant-shear and flexural bonding tests.

The study presents an experimental method to investigate the mechanical behavior of two fiber-reinforced repair mortars. Section 2 describes the different mortars studied and the samples preparation. A summarize of characteristics of these mortars in terms of shrinkage, porosity, cement hydration, and other material properties is also given in section 2. Section 3 gives a description of the compression, three-point bending and tensile tests. The results obtained are presented in Section 4, followed by a discussion of the behavior observed. Bond characterization between substrate and repair mortars is presented and discussed in section 5.

## 2. Materials and sample preparation

Two fiber-reinforced repair mortars were used, together with an ordinary mortar, which it was used to provide control samples for comparison and to replace the substrate for bond tests. Details of the repair materials are as follows (Table1):

FLM is a Fiber-reinforced Lime-based Mortar, which consists of sand, limestone, special hydraulic binder, lime, polyacrylonitrile fibers, thickening agent and additives. FLM resists sea and sulphated water. A water/powder ratio of 0.22 is used.

FOM is a non-shrinkable Fiber reinforced Ordinary Mortar, which contains sand, ordinary cement, polyacrylonitrile fibers, silica fume and additives. FOM resists carbonation, sea and sulphated water. A water/powder ratio of 0.14 is used.

OM is ordinary mortar prepared using CEMII 32.5R cement. The mix proportions (by weight) were 1 : 3.68 : 0.48 (cement : sand : water), to achieve 28 days strength of 25 MPa and of 20 GPa Young modulus. The porosity of the 28-days old mortars was obtained by Mercury intrusion porosimetry. Table 1 regroups some physical properties of the mortars.

Compression test samples were cast in 40 mm diameter and 80 mm height cylindrical mould. Flexural samples were cast in 40x40x160 mm<sup>3</sup> prismatic mould. All samples were cast in three layers on a vibrating table (50 Hz, 2 layers, 10 s/layer) and cured in the atmosphere of the laboratory for 24 hours. Then, the samples were removed from the mould and stored in a relatively dry atmosphere (23 °C and 50% RH). The slant-shear test substrates were cast in 40 mm diameter and 80 mm height half-cylindrical mould with the interface line at 30° to the vertical. Flexural bonding samples were cast in 40x40x160 mm<sup>3</sup> moulds and then cut in two halves by a diamond saw. Surfaces are treated to obtain various roughness. Four surface preparation methods were used to obtain smooth grounded, hand-engraved, steel-brushed/sand-blasted and as broken surfaces. For the slant-shear tests, only the three first surface types were used. After the preparation of the surfaces, the substrates were stored under four moisture conditions to obtain dry substrate with dry surface, wet substrate with dry surface, saturated substrate with dry surface and saturated substrate with saturated surface. Only wet substrates with dry surfaces were used for flexural bonding tests. The samples were cured in the atmosphere of the laboratory for 24 h. Then, they were removed from the moulds and stored in a relatively dry atmosphere (23 °C and 50% RH) for 28 days.

### 3 Experimental tests

#### 3.1. Three-point bending tests

A sketch of the experimental setup is given in figure 1. The three-point bending tests were performed on the  $40 \times 40 \times 160 \text{ mm}^3$  samples, using an INSTRON 4505 type machine equipped with a 5 kN load cell and a PID servo control. A strain measurement was achieved on the face under tensile stress using an INSTRON extensometer put in the middle of the sample. The PID servo control allowed us to rule the tests under strain control conditions. The tests were carried out on mortars at various ages between 7 and 210 days. At least five samples were tested for each age. Figure 1 shows a typical load versus tensile strain diagram. The ascending part of the curve is quasi-linear. However, near the top of the curve, the slope exhibits a slight decrease which indicates the damage initiation. At peak load, the micro-cracks coalesce into an unstable crack. The decreasing part of the curve corresponds to the propagation of this crack, which induces a loss of sample stiffness. Various parameters are used for our comparisons: the maximum load  $F_{max}$  applied to the sample over the test, the strain at peak load  $\epsilon^{peak}$  associated with  $F_{max}$ , the initial sample stiffness  $K_0$ .

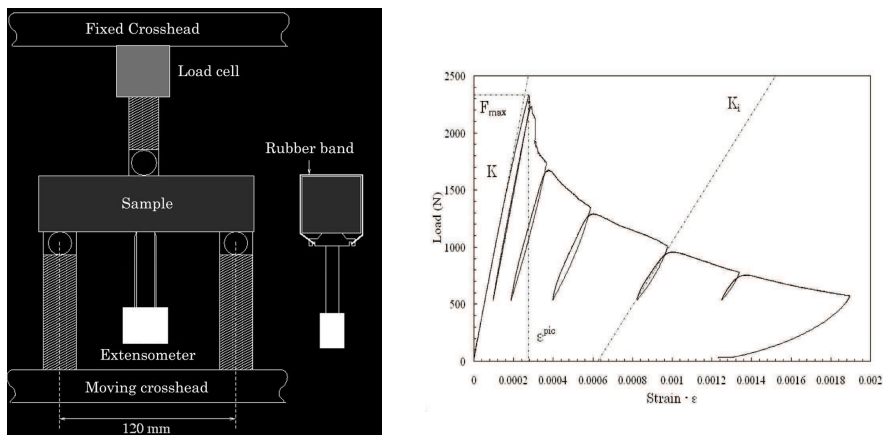


**Figure 1.** Experimental setup for three-point bending test and typical load strain curve.

#### 3.2. Uniaxial tensile tests

Tensile tests were carried out on samples with cylindrical central gauge zone (40 mm diameter, 30 mm height) using the same machine as the three-point bending tests. Two INSTRON extensometers were mounted on the opposite sides of the sample for strain measurement as well as for test control. A *Modified-tensile test* (figure 2), was performed using hollow samples. In the 14 mm diameter hole, which

is obtained by molding, we introduce a 12 mm diameter brass bar. Tension load is applied directly to the bar ends and pip-caps glued on the sample ends. An adaptive control mode was used to achieve *modified-tensile test*. For these tests, tensile stress in the mortar sample  $\sigma_M$  can be determined by the following equation:

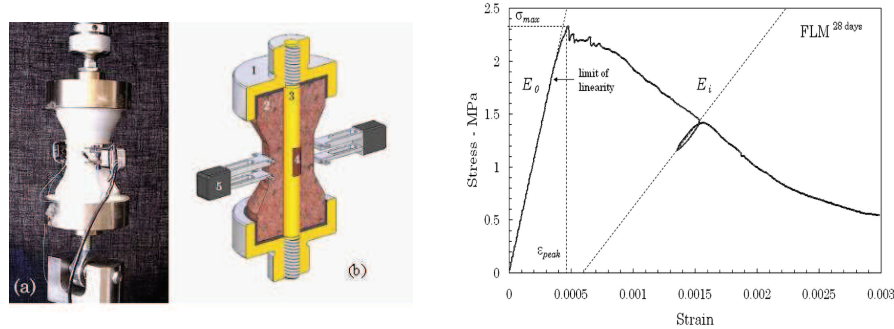


**Figure 2.** Modified tensile test setup (1 steel pip caps, 2 sample, 3 metallic brass, 4 strain gauge, 5 extensometers) and complete stress strain curve.

Where  $E_B$  is the Young's modulus of the bar, obtained by direct tensile test.  $F_{tot}$  is the load applied to the composite sample (mortar sample and brass bar).  $\mathcal{E}_B$  is the strain measured in bar by two strain gauges fixed on the opposite sides in the middle of the bar.  $\mathcal{E}_M$  is the strain of the mortar obtained by the extensometers.  $S_B$  and  $S_M$  are the sections of the bar and the mortar sample respectively. More details of *modified-tensile test* can be found in Pascal *et al.* (2004) and Mallat *et al.* (2011).

Figure 2 shows a complete stress-strain curve of FLM obtained by *modified tensile test*. The decrease of the slope on the ascending curve indicates the damage initiation.

#### 4 Results and discussions

Figure 3 and 4 show the envelope of load-strain curves (a) and the peak load *versus* the age of the repair mortars (b), obtained by three-point bending tests. FLM maximum load increases with time, however the mortar becomes more brittle; at 210 days mortar age, FLM samples fail brutally and it was difficult to obtain complete post-peak response by three-point bending test. The embrittlement of the FLM with time is confirmed. FOM flexural strength increases until 28 days and decreases beyond this age. The reasons accounting for the evolution of the flexural strength are not obvious. First of all, the porosity can play a major role, since the volume fraction of pores is not similar throughout the materials. We know that cement hydration strengthens the cement-based materials by filling the capillary pores with hydrates, especially during the first month after their making (Folliot and Buil

1982). The influence of a possible difference in cement hydration is not easy to handle. The cement hydration in the materials may be responsible for the bending strength evolution. Nevertheless, this is true for the FLM but not for the FOM. Cement hydration is not the only cause of the bending strength evolution presented in figure 3. The last reason we consider is the percolation of the thickening agent over the FLM samples (figure 4). A film rich in thickening agent is formed on the FLM sample faces. SEM observations achieved on the FLM sample faces revealed this film although EDS elementary analysis did not identify its precise nature. This film may limit the FLM sample from drying out and, therefore, from surface micro-cracking. On the contrary, micro-cracks on the skin of the FOM sample, due to sample drying out, would be responsible for the damage initiation (Pascal *et al.* 2004, Li *et al.* 2001).

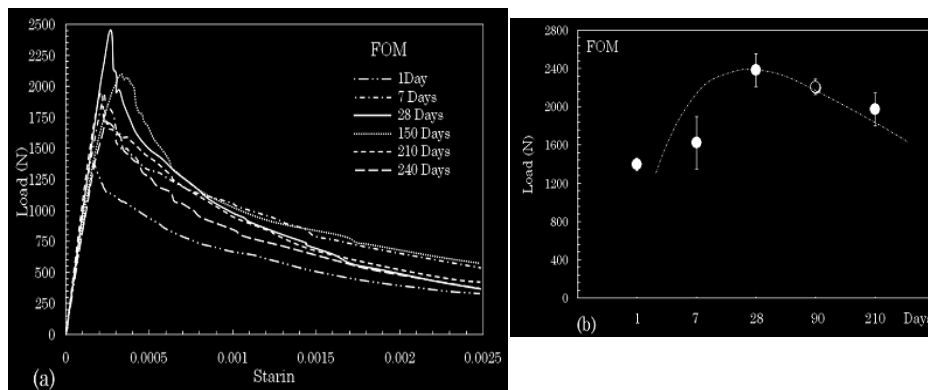


Figure 3. Load-strain curves (a) and evolution of flexural load (FOM).

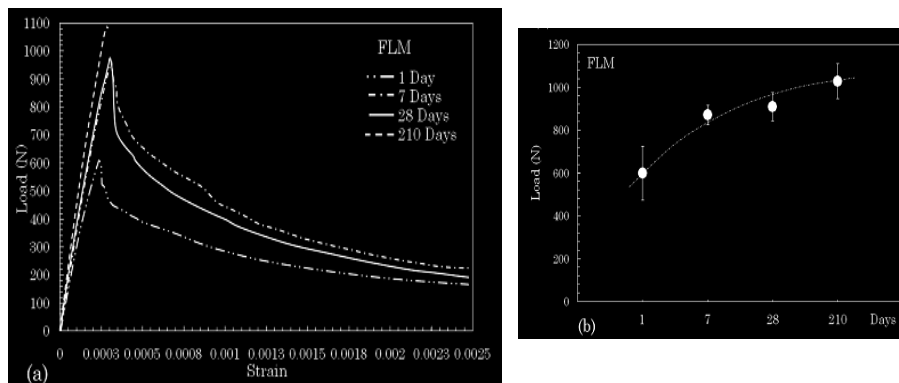
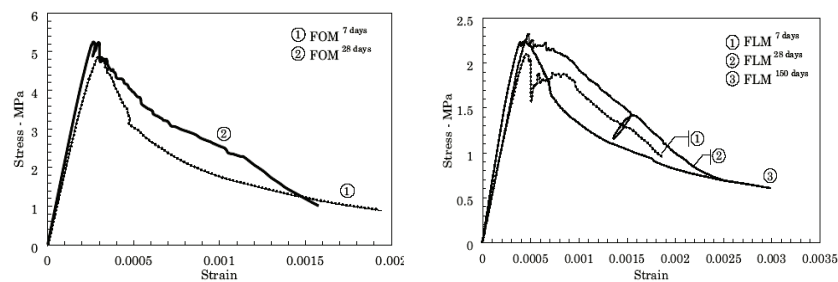


Figure 4. Load-strain curves (a) and evolution of flexural load (FLM).

Figure 5 shows stress-strain curves of the mortars obtained at various ages by *modified tensile tests*. The highest tensile strength was accorded to the mortar containing silica fume (FOM). In addition, silica fume has increased the tensile strain capacity of the FOM compared with an ordinary mortar having similar Young's modulus. The role of silica fume to increase the tensile strength is known (Jolio and al., Emmons 1994). Although FOM tensile strength is higher than that of the FLM, however its strain at peak is lower. The highest tensile strain capacity of the FLM may be justified by its microstructure and/or the percolation of thickening agent in the matrix. Tensile tests have also allowed us to study the evolution of materials. Both Young's moduli and tensile strengths of the materials increase with time. FLM evolve very slowly between 7 and 28 days (Fig. 5), which is due to the slow carbonation and hydration processes of the mortar, significant increase of Young's modulus is observed at 150 days age.



**Figure 5.** Stress-strain tensile curves for FOM and FLM.

## 5 Bond characterization

FOM has the highest bond strength in both slant-shear and flexural bonding tests (figure 6). Slant-shear samples with engraved surface produced the highest bond strengths. Grounded (smooth) surface produced the lowest bond strengths. Slant-shear test results show also that wet or saturated substrates with dry surfaces gave the highest bond strengths compared with the other moisture conditions. Emmons (1994) mentions that the moisture level of the substrate may be critical in achieving bond. He states that an excessively dry substrate may absorb too much water from the repair material while excessive moisture in the substrate may clog the pores and prevent absorption of the repair material. Therefore, a saturated substrate with a dry surface is considered to be the best solution. Chorinsky (1996) concluded that too dry or too wet surface of concrete substrate always results in weak bond strength of the interface. All FOM-to-substrate samples, except for those with broken surface substrate, underwent a monolithic behavior (figure 7), contrary to FOM-to-broken

surface substrate samples which especially debonding at high level of load occurred. Debonding also occurred for all FLM-to-substrate samples.

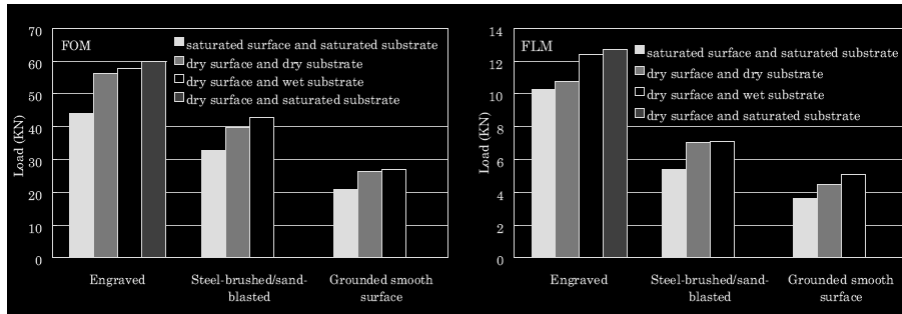


**Figure 6.** Influence of moisture condition and surface roughness on shear bonding strength

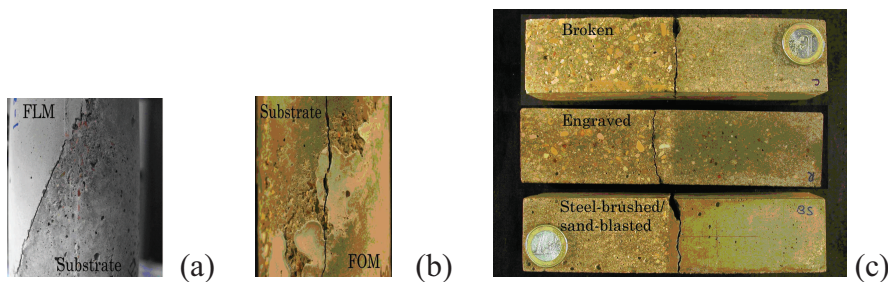


**Figure 7.** Failure mode of repair mortars-to-substrate samples by slant shear test (a) and (b) and flexural test (c)

For the flexural bonding tests, all substrates were saturated with dry surfaces. FOM to engraved substrate surface produced the highest bond strength. However, the same surface type produced the lowest bond strength in the case of FLM, which indicates that the bonding behavior of different materials may change even if they are applied on the same type of surface. In addition, bond strength values of FOM to substrate were between the flexural strength values of the two basic mortars (FOM and substrate (figure 8)). This is not true for the FLM where the bond strength values were lower than the flexural strength values of the basic mortars (figure 8). It shows the repair mortars-to-substrate interfacial zone. Figure 8 highlights an obvious separations between substrate and FLM accompanied by a high concentration of micro-cracks in the matrix. The micro-cracks are orthogonal to the sand grains and they are probably induced by the great shrinkage of the paste. SEM observations also show many large interfacial transition zones resulting from weak bond between paste and aggregates. Shrinkage cracking exists at all repair interfaces due to differential shrinkage between the hardened substrate and the freshly laid plastic



overlay. Under an applied load, these flaws cause stress concentrations and render the interface weak. This is the case of the FLM: significantly pronounced shrinkage cracking may be expected to occur at the repair interface. The low bond strength between substrate and FLM may also be related to the presence of the thickening agent in the mortar. In this case, a film rich in thickening agent may be formed at the interface and the bond of new-to-old mortar depends mainly on glutinous nature of the thickening agent (molecular force). Finally, the high content of large portlandite crystals between the film and the matrix weakens this zone. The failure will probably occur through this zone. The interfacial zone of FOM-to-substrate is more dense and uniform, and few cracks and interfacial transition zones were observed (Fig.13): chemically, the silica fume reacts pozzolanically with calcium hydroxide produced by the hydration of cement to produce a greater solid volume of calcium silicate hydrate gel, leading to an additional reduction in capillary porosity and decreases the calcium hydroxide (weak large crystal) content in the matrix Chorinsky 1996, Li and Xiong 2001, Jolio and al. 2004). Physically, the numerous silica fume particles in the FOM fill the weak spaces of interfacial and interfacial transition zones making them denser and more homogeneous. The good bond between FOM paste and sand grains prevents the propagation of cracks through the transition zone.

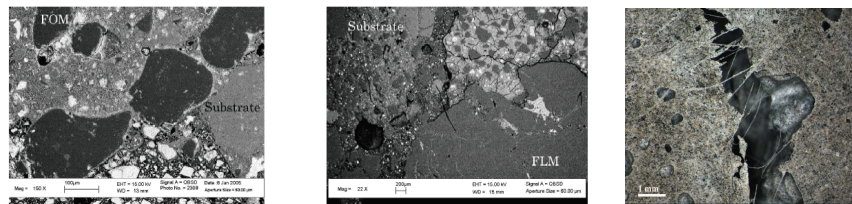


**Figure 8.** Back scattered electron SEM micrograph of interfacial zones of repair mortars 90 days old-to-substrate 80 years old and fiber bridging over crack.

## 6 Conclusion

The test results described in this paper indicate that synthetic fibers and thickening agent would not modify the nature of the cement hydration products. The slow carbonation of portlandite and the thickening agent slow down the evolution of the Fiber-reinforced Lime-based mortar (FLM) mechanical properties. The flexural strength of Fiber-reinforced Ordinary Mortar (FOM) increases until 28 days and decreases after this age. The FLM flexural strength remains increasing with time. The increase of the FLM flexural strength and the presence of thickening agent in the mortar match. Since the influence of porosity is difficult to verify and a difference in cement hydration cannot explain this evolution, it is suggested that the percolation of the thickening agent over the sample increases its flexural strength. The thickening agent may prevent the material from skin micro-cracking which could be the cause of the early damage initiation into the mortar. On the contrary,

micro-cracks on the skin of the FOM sample, due to sample drying out, would be responsible for the damage initiation. Tensile tests results show that fibers and silica fume enhance the tensile strength and strain capacity of mortars.

The bonding test results show that both surface roughness and moisture conditions of substrate has a significant influence on the bond strength even if the FLM is less sensitive to surface type. Microcracking due to differential shrinkage between substrate and FLM weakens the bond and induces a lower failure load. However, silica fume in the FOM increases the mechanical properties of the repair mortar-to-substrate interfacial zone and interfacial transition zones, thus leading to a better bond.

## 7. References

- Bhandja S., Sengupta B. Influences of silica fume on the tensile strength concrete. *Cement and concrete Research* 2005; 35: 743-747.
- Chorinsky E. G. F. Repair of concrete floors with polymer modified cement mortars. *RILEM Symposium Adhesion between polymers and concrete*. Chapman and Hall, London. 1996: 230-234.
- Emberson N. K., Mays G. Significance of property mismatch in the patch repair of structural concrete. Part I; *Magazine of Concrete Research* 1990; 42:147-160.
- Emmons P. H. Bonding repair materials to existing concrete. *Concrete repair and maintenance*. M. A. R.S. Means Company 1994:154-163.
- Folliot A., Buil L La structuration progressive de la Pierre de ciment, in: *Le béton hydraulique: connaissance et pratique*. Presse de l'ENPC. Paris 1982.
- Jolio N. B. S., Branco A. B. F., Vitor D. S. Concrete-to-concrete bond strength, influence of the roughness of the substrate surface. *Construction and Building Materials* 2004; 18: 675-681.
- Li G., Xie H., Xiong G. Transition zone studies of new-to-old concrete with different binders. *Cement and Concrete Composites* 2001; 23: 381-387.
- Mallat A., Alliche A. Physico-chemical and mechanical behaviour of fiber reinforced repair mortars. *Third International Conference on FRP composites in civil engineering (CICE 2006)*, Miami, USA, Dec. 2006.
- Mallat A. *Phénomènes de dégradation des ouvrages anciens, techniques et matériaux de rehabilitation*. Thèse Ecole Centrale de Paris. Juin 2008.
- Mangat P., Limbachiya M. Repair material properties for effective structural application. *Cement and concrete Research* 1997; 27: 601-617.
- PascalS., Alliche A., Pilvin P. Mechanical behaviour of polymer modified mortars. *Materials Science and Engineering A*. 2004: 380: 1-8.